

Self-Training Boosted Multi-Faceted Matching Network for Composed Image Retrieval

Haokun Wen, Xuemeng Song, *Senior Member, IEEE*, Jianhua Yin, *Member, IEEE*, Jianlong Wu, *Member, IEEE*, Weili Guan, *Member, IEEE*, Liqiang Nie, *Senior Member, IEEE*

Abstract—The composed image retrieval (CIR) task aims to retrieve the desired target image for a given multimodal query, *i.e.*, a reference image with its corresponding modification text. The key limitations encountered by existing efforts are two aspects: 1) ignoring the multi-faceted query-target matching factors; 2) ignoring the potential unlabeled reference-target image pairs in existing benchmark datasets. To address these two limitations is non-trivial due to the following challenges: 1) how to effectively model the multi-faceted matching factors in a latent way without direct supervision signals; 2) how to fully utilize the potential unlabeled reference-target image pairs to improve the generalization ability of the CIR model. To address these challenges, in this work, we first propose a multi-faceted Matching Network (LIMN), which consists of three key modules: multi-grained image/text encoder, latent factor-oriented feature aggregation, and query-target matching modeling. Thereafter, we design an iterative dual self-training paradigm to further enhance the performance of LIMN by fully utilizing the potential unlabeled reference-target image pairs in a semi-supervised manner. Specifically, we denote the iterative dual self-training paradigm enhanced LIMN as LIMN+. Extensive experiments on three real-world datasets, FashionIQ, Shoes, and Birds-to-Words, show that our proposed method significantly surpasses the state-of-the-art baselines.

Index Terms—Composed Image Retrieval, Multimodal Retrieval.

1 INTRODUCTION

IMAGE retrieval has been a cardinal task in computer vision and database management domains since the 1970's [1]. It has laid the foundation and paved the way for a wide range of applications, such as face recognition [2], [3], fashion retrieval [4], and person re-identification [5], [6]. Traditional image retrieval paradigms allow users to deliver their search intentions by either pure text queries or image queries. However, in many cases, the user's search intention is sophisticated, and cannot be well delivered by the single-modal query. Accordingly, to facilitate the flexible expression of users' search intentions, Vo *et al.* [7] first proposed the task of composed image retrieval (CIR), where the input query is composed of a reference image and a modification text describing the user's modification demands towards the reference image. As CIR has great potential value in many real-world applications, such as commercial product search and interactive intelligent robots, it has gained increasing research attention in recent years.

Although the pioneer research studies [8]–[18] have achieved promising progress, they have two key limitations.

L1: Ignore the multi-faceted query-target matching factors. As shown in Figure 1, for evaluating whether the target image matches the multimodal query, we usually

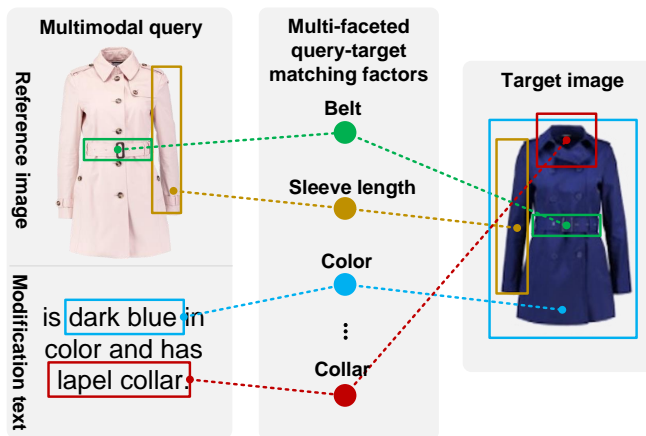


Fig. 1. An example of the multi-faceted query-target matching factors between the multimodal query and the target image. Note that semantics like “color” or “belt” only convey a concept since the matching factors are implicitly contained.

need to consider multiple factors (*e.g.*, the color, collar, and sleeve length). Nevertheless, none of the existing efforts take this into consideration. The previous studies simply represent the multimodal query and the target image by a single overall vector, respectively, based on which they conduct the query-target matching. Apparently, this strategy fails to clearly model the various latent factors affecting the query-target matching evaluation and inevitably leads to suboptimal performance.

L2: Ignore the potential unlabeled reference-target image pairs in the existing benchmark dataset. Samples in the existing CIR datasets are all in the form of triplet <reference image, modification text, target image>. In particular, the reference-target image pairs are obtained

- H. Wen, J. Wu, and L. Nie are with the School of Computer Science and Technology, Harbin Institute of Technology (Shenzhen), 518055, China. E-mail: whenhaokun@gmail.com, jtwu1992@pku.edu.cn, nieliqiang@gmail.com.
- X. Song and J. Yin are with the School of Computer Science and Technology, Shandong University, Tsingtao, 266000, China. E-mail: sxmustc@gmail.com, jhyin@sdu.edu.cn.
- W. Guan is with the Department of Data Science and Artificial Intelligence, Monash University, Clayton, 3800, Australia, and also with the AI Research Center, Pengcheng Laboratory, Shenzhen, 518055, China. E-mail: honeyguan@gmail.com.

X. Song and L. Nie are the corresponding authors.

in a heuristic manner, while the modification text is human-annotated. Apparently, creating such training samples is expensive and laborious, which largely limits the size of the benchmark datasets. Simply relying on the limited samples in existing benchmark datasets, previous research efforts encountered the overfitting problem to some extent and suffered from poor generalization ability. In fact, we observed that there are still plentiful potential unlabeled reference-target image pairs in the dataset being untapped by previous work, which are highly similar with few different properties.

Overcoming the flaws mentioned above is non-trivial due to the following two challenges. 1) Each factor that affects the query-target matching evaluation should emphasize its correlated features of the multimodal query and the target image. For example, for the evaluation on the “belt” factor, we should pay attention to the middle region features of the images or the related keywords in the modification text. Meanwhile, we do not have direct supervision signals for learning the multi-faceted query-target matching factors. Therefore, how to effectively model the multi-faceted query-target matching factors in a latent way constitutes the first challenge. 2) Although a number of potential unlabeled reference-target image pairs can be heuristically uncovered from the benchmark dataset, they cannot be used directly for training the CIR model since they lack the corresponding modification text. Accordingly, another tough challenge is how to fully utilize the potential unlabeled reference-target image pairs in a semi-supervised manner to improve the generalization ability of the CIR model.

To address the challenges mentioned above, we first propose a multi-faceted Matching Network, LIMN for short, to model the multi-faceted query-target matching factors between the multimodal query and the target image. Thereafter, we devise a customized iterative dual self-training paradigm to make full use of the potential unlabeled reference-target image pairs and solve the task in a semi-supervised manner. We name the iterative dual self-training paradigm enhanced LIMN as LIMN+.

For LIMN, it contains three vital modules: multi-grained image/text encoder, latent factor-oriented feature aggregation, and query-target matching modeling. The first module is committed to extracting the multi-grained visual and textual features of the image and the text in the training triplets. In the second module, we introduce multiple matching tokens to model the latent multi-faceted query-target matching factors, each of which is responsible for capturing a latent matching factor. In particular, we utilize the standard Transformer [19] architecture to aggregate the related features for each matching token, where the intra- and inter-interaction among different inputs (e.g., reference image, modification text, and matching tokens) can be fully explored. In the third module, apart from the conventional commonly used batch-based classification loss for making the learned matching tokens that have aggregated related features from the multimodal query and the target image close, we also design a factor-orthogonal regularization to ensure that different matching tokens capture different matching factors.

As for LIMN+, the key novelty lies in our proposed iterative dual self-training paradigm. It takes full advantage

of the existing image difference captioning (IDC) [20] model that can generate a natural language-based text to describe the difference between two images. Specifically, our iterative dual self-training paradigm utilizes the IDC model to automatically annotate the potential unlabeled reference-target image pairs and produce pseudo triplets for enhancing the training of the LIMN model. Conversely, the well-trained LIMN model can measure the quality of the pseudo triplet by evaluating its query-target matching score and determine whether the pseudo triplets can be used. Through iterative cooperation learning, the performance of LIMN gets improved.

Our main contributions can be summarized as follows:

- As far as we know, we are the first to explore the latent multi-faceted query-target matching factors in the context of CIR. In particular, we propose a multi-faceted matching network, whose novelty mainly lies in the latent factor-oriented feature aggregation for the query and target.
- To the best of our knowledge, we are the first to dissect the scarce dataset problem encountered by the CIR task. Specifically, we design an iterative dual self-training paradigm to make full use of the potential unlabeled reference-target image pairs and further boost the CIR performance. The paradigm is hot-plugging and is applicable to any other existing CIR methods.
- Extensive experiments on three real-world datasets demonstrate the superiority of our proposed models (LIMN and LIMN+). As a byproduct, we released the source code to facilitate the research community¹.

The remainder of the paper is organized as follows. Section 2 briefly reviews the related work. In Section 3, we detail the proposed LIMN and iterative dual self-training paradigm. The experimental results and analyses are presented in Section 4, followed by the conclusion and future work in Section 5.

2 RELATED WORK

Our work is closely related to the studies on composed image retrieval (CIR) and self-training.

2.1 Composed Image Retrieval

Recent years have witnessed growing research interest in CIR due to its theoretical significance of research and potential commercial value. There are various efforts [7]–[11], [13], [15]–[18], [21] that attempt to tackle this task. For instance, Vo *et al.* [7] first proposed a gating and residual module to compose the multimodal query features, where the reference image is adaptively preserved and transformed to derive the composed query representation. Following that, Chen *et al.* [8] resorted to the attention mechanism to fuse the hierarchical reference image features with the modification text feature. Later, Kim *et al.* [16] presented a refined version of TIRG [7] to fuse the multi-granularity features of the reference image and modification text. Thereinto, a correction network on the difference between the reference image and target image is introduced to further

1. <https://anosite.wixsite.com/limn>.

regularize the fusion results. Moreover, Wen *et al.* [10] utilized a fine-grained local-wise composition module and a fine-grained global-wise composition module, which can model the diverse modification demands more precisely. Thereafter, Lee *et al.* [13] first adopted a content modulator to perform local updates of the reference image according to the modification text, and then applied a style modulator to achieve the global modification.

Although these methods have made prominent progress, they overlook the multi-faceted factors that affect the matching evaluation between the multimodal query and the target image in the context of CIR, and inevitably obtain the suboptimal retrieval performance. In addition, the existing efforts ignore the potential unlabeled reference-target image pairs in the existing benchmark dataset. Beyond these studies, in this work, we captured the multi-faceted query-target matching factors by introducing multiple matching tokens to achieve promising retrieval performance. Besides, we designed an iterative dual self-training algorithm to make full use of the potential unlabeled reference-target image pairs and relieve the problems caused by limited data size, and consequently achieved promising results in CIR.

2.2 Self-training

Self-training is one of the earliest techniques in semi-supervised learning [22]. Typically, by self-training, a model is first trained under the supervision of the labeled data. And then the well-trained model is employed to label the unlabeled data to derive the pseudo labeled data. Finally, both the labeled and the pseudo labeled data are jointly utilized to train another model, which can yield better performance. The advantage of self-training is that it can adapt the supervised model to function in a semi-supervised manner and learn from the unlabeled data. This strategy is simple yet effective and has drawn many researchers' attention. For example, Xie *et al.* [23] utilized the self-training technique to significantly advance the image classification accuracy by adding noise such as dropout, stochastic depth and data augmentation to the combination of the labeled and the pseudo labeled data. In addition, Ye *et al.* [24] adopted self-training in zero-shot text classification, where a reinforced learning framework is proposed to select more reliable data samples automatically. Moreover, Yang *et al.* [25] employed self-training in semi-supervised object detection, in which the non-maximum suppression is utilized to fuse the detection results from different iterations and the performance is further improved.

Inspired by these successful applications of self-training, in this work, we adapted the self-training technique to the CIR task to alleviate the limited dataset problem. Considering the setting of CIR, we adopted an image difference captioning model to produce pseudo triplets for promoting the performance of the CIR model.

3 METHODOLOGY

In this section, we first formulate the research problem and then elaborate on the proposed muLTI-faceted Matching Network (LIMN), followed by the iterative dual self-training paradigm.

3.1 Problem Formulation

In this work, we aim to tackle the task of CIR, whose goal is to retrieve the target images that meet the multimodal query (*i.e.*, a reference image and a modification text). Suppose we have a set of N training triplets, denoted as $\mathcal{T} = \{(x_r, t_m, x_t)\}_{i=1}^N$, where x_r , t_m , and x_t refer to the reference image, modification text, and target image, respectively. Essentially, we aim to learn an embedding space where the representations of the multimodal query (x_r, t_m) and corresponding target image x_t should be as close as possible, which can be formally expressed as follows,

$$\mathcal{H}(x_r, t_m) \rightarrow \mathcal{H}(x_t), \quad (1)$$

where \mathcal{H} denotes the to-be-learned mapping function for embedding both the multimodal query and the target image. Here we utilize the same mapping function to ensure the representations of the multimodal query and the target image lying in the same semantic embedding space.

3.2 LIMN

One major novelty of our work is that we take the multiple factors influencing the matching evaluation between the multimodal query and the target image into account. Specifically, we propose a muLTI-faceted Matching Network (LIMN), as shown in Figure 2. It consists of three key modules: (a) multi-grained image/text encoder, (b) latent factor-oriented feature aggregation, and (c) query-target matching modeling. First, the visual images (including the reference image x_r and the target image x_t) and textual modification (t_m) are encoded by the multi-grained image encoder and text encoder, respectively (detailed in Section 3.2.1). Second, the multi-grained representations of the multimodal query and the target image are aggregated by a Transformer, respectively, where the latent multi-faceted query-target matching factors are modeled (explained in Section 3.2.2). Finally, a conventional ranking loss and a newly devised factor-orthogonal regularization are jointly utilized to optimize our model LIMN (described in Section 3.2.3). We now elaborate each module in LIMN as follows.

3.2.1 Multi-grained Image/Text Encoder

Existing efforts [10], [12], [16] have corroborated that utilizing multi-grained visual and textual features can promote the performance of CIR. Inspired by this, we extract both local and global representations for the reference image and target image, as well as both word-level and sentence-level representations for the modification text.

Multi-grained Image Encoder. Towards the image encoding, we employ the ImageNet [26] pre-trained ResNet50 [27], which has been widely used as the image encoder for the CIR task [8], [10], [13], [16], [28]. As the reference image and the target image share the same visual feature extraction process, we here take that of the reference image as an example.

Regarding the local visual feature, we choose the feature maps output by the second-to-last layer of ResNet, where each spatial entry of the feature maps can deliver discriminative information about specific image regions [29]. Let $\mathbf{X}_r'' \in \mathbb{R}^{C \times H \times W}$ denote the feature maps generated by the second-to-last layer of ResNet for the reference image,

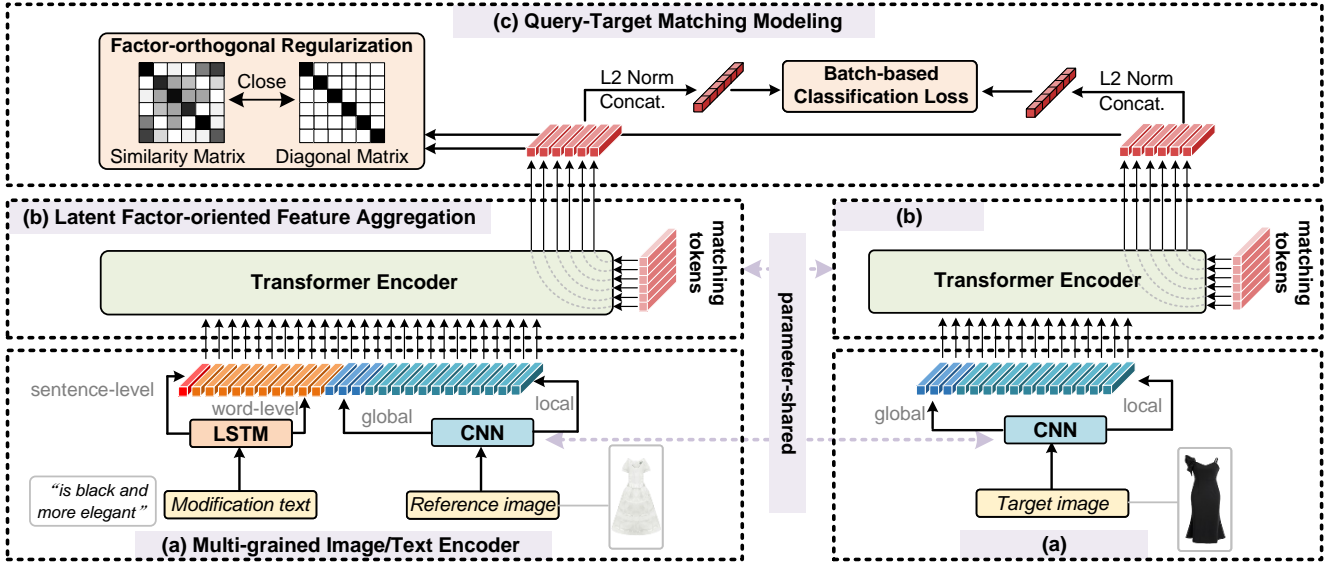


Fig. 2. Illustration of our proposed LIMN. It consists of three modules: (a) multi-grained image/text encoder, (b) latent factor-oriented feature aggregation, and (c) query-target matching modeling.

where C is the channel dimension, and $H \times W$ refers to the resolution of feature maps. We first line up \mathbf{X}_r' to a sequence by their positions following [30], denoted as $\bar{\mathbf{X}}_r'' \in \mathbb{R}^{C \times (H \times W)}$, and then apply a fully connected layer to derive the local visual feature of the reference image. Formally, we have,

$$\mathbf{E}_r^L = \text{FC}_I^L(\bar{\mathbf{X}}_r''), \quad (2)$$

where $\mathbf{E}_r^L \in \mathbb{R}^{D \times (H \times W)}$ is the extracted local visual feature of the reference image.

As for obtaining the global visual feature, we utilize the feature maps yielded by the last layer of ResNet, since we argue that the deeper the network, the larger the receptive field of the convolution operation, and the more abstract the extracted features. To endow the global visual feature able to encode various overviews of the image, we utilize three commonly used pooling strategies, *i.e.*, max pooling, average pooling, and gem pooling [31], to derive the global visual feature. Formally, for the reference image feature maps \mathbf{X}_r' generated by the last layer of ResNet, we have,

$$\mathbf{E}_r^G = \text{FC}_I^G([\text{Max}(\mathbf{X}_r'); \text{Avg}(\mathbf{X}_r'); \text{Gem}(\mathbf{X}_r')]), \quad (3)$$

where $\mathbf{E}_r^G \in \mathbb{R}^{D \times 3}$ is the global visual feature of the reference image, $\text{Max}(\cdot)$, $\text{Avg}(\cdot)$, and $\text{Gem}(\cdot)$ refer to different pooling strategies. $[\cdot]$ denotes the concatenate operation and FC_I^G is the fully connected layer to ensure that the local and global feature dimensions are aligned.

Afterwards, we concatenate the local visual feature and global visual feature of the reference image to derive its final visual representation as follows,

$$\mathbf{E}_r = [\mathbf{E}_r^L; \mathbf{E}_r^G], \quad (4)$$

where $\mathbf{E}_r \in \mathbb{R}^{D \times (H \times W + 3)}$ denotes the visual representation of the reference image. The visual representation of the target image $\mathbf{E}_t \in \mathbb{R}^{D \times (H \times W + 3)}$ can be obtained in the same way.

Multi-grained Text Encoder. For the text encoding, following previous efforts [7], [8], [10], we utilize a single-layer long short-term memory network (LSTM) [32] as the multi-grained text encoder. Specifically, the modification text is first tokenized into a token sequence and then fed into the LSTM as follows,

$$\mathbf{T}_m = [\mathbf{t}_1, \dots, \mathbf{t}_K] = \mathcal{F}_{\text{LSTM}}(t_m), \quad (5)$$

where $\mathbf{t}_i \in \mathbb{R}^{D_t}$ is the hidden state output of the i -th word, $\mathbf{T}_m \in \mathbb{R}^{D_t \times K}$ denotes the hidden state output of the given modification text yielded by the LSTM, D_t is the feature dimension and K is the text length.

Similar to the multi-grained visual encoding, we jointly consider the word-level and sentence-level representations of the modification text. Specifically, for the word-level representation, we apply a fully connected layer to the hidden state output of the words in the modification text as follows,

$$\mathbf{E}_m^W = \text{FC}_M^W(\mathbf{T}_m), \quad (6)$$

where $\mathbf{E}_m^W \in \mathbb{R}^{D \times K}$ denotes the word-level representation of the modification text. As for the sentence-level representation, we employ another fully connected layer to the hidden state output of the last word in the modification text as follows,

$$\mathbf{E}_m^S = \text{FC}_M^S(\mathbf{t}_K), \quad (7)$$

where $\mathbf{E}_m^S \in \mathbb{R}^D$ is the sentence-level representation of the modification text. Thereafter, we concatenate them to obtain the final textual representation of the modification text as follows,

$$\mathbf{E}_m = [\mathbf{E}_m^W; \mathbf{E}_m^S], \quad (8)$$

where $\mathbf{E}_m \in \mathbb{R}^{D \times (K+1)}$ denotes the final representation of the modification text.

3.2.2 Latent Factor-oriented Feature Aggregation

In this work, beyond previous studies, we explore the latent multi-faceted query-target matching factors that affect the matching evaluation between the multimodal query and the target image. To fulfil this, supposing there are U query-target matching factors, we introduce U matching tokens, each of which endeavors to capture a latent factor. Each matching token is responsible for adaptively aggregating features of the multimodal query/target image according to its corresponding factor. For example, in Figure 1, the matching token that ought to capture the ‘‘belt’’ factor should aggregate the related features of the belt from the multimodal query and the target image, respectively. Specifically, we assign each matching token a learnable vector. Accordingly, the U matching tokens can be denoted as $\mathbf{E}_p \in \mathbb{R}^{D \times U}$, *i.e.*, a learnable matrix, which is randomly initialized and will be optimized during the training process. D is the feature dimension, which is equal to that of the visual and textual representations. Each column of \mathbf{E}_p corresponds to a latent factor.

We then utilize an off-the-shelf Transformer encoder [19], which can model a comprehensive interaction among the inputs by virtue of self-attention mechanism, to aggregate the related features into the corresponding matching tokens. Specifically, we first concatenate the representation of matching tokens with that of the multimodal query and the target image, respectively, which is given as,

$$\begin{cases} \Phi_q = [\mathbf{E}_r; \mathbf{E}_m; \mathbf{E}_p], \\ \Phi_t = [\mathbf{E}_t; \mathbf{E}_p], \end{cases} \quad (9)$$

where $\Phi_q \in \mathbb{R}^{D \times (H*W+K+4+U)}$ and $\Phi_t \in \mathbb{R}^{D \times (H*W+3+U)}$ denote the concatenated query input and the target input, respectively. We then feed Φ_q and Φ_t into the Transformer encoder as follows,

$$\begin{cases} \Psi_r = \mathcal{F}_{\text{Transformer}}(\Phi_r), \\ \Psi_t = \mathcal{F}_{\text{Transformer}}(\Phi_t), \end{cases} \quad (10)$$

where $\Psi_r \in \mathbb{R}^{D \times U}$ and $\Psi_t \in \mathbb{R}^{D \times U}$ denote the updated matching token matrices, which have aggregated the necessary features from the multimodal query and the target image, respectively. Note that we do not add additional positional encodings or modality type encodings to the query input and target input, due to two major concerns. 1) The visual representations of query and target images are extracted by CNNs, and it has been corroborated that CNNs can implicitly encode space information [33]. 2) The visual representations, textual representation, and matching token representations are initialized in different ways, *i.e.*, CNN, LSTM, and random initialization, respectively. Thus, they are inherent with different semantics and do not need additional encodings to be differentiated. It is also worth noting that the parameters of the Transformers that process the query input Φ_q and target input Φ_t are shared. The underlying philosophy is to make the output embeddings of both ends still remain in the same semantic space, which facilitates the following query-target matching modeling.

The advantages of using Transformer to perform the latent factor-oriented feature aggregation can be summarized into two-folds. 1) The self-attention mechanism in the Transformer encoder can comprehensively model the interactions

among representations of the multimodal query, the target image, and the matching tokens. Specifically, both the intra-interactions among representations of the same subject (*e.g.*, the multi-grained representations of the reference/target image or the representations of the matching tokens) and the inter-interactions among representations of different subjects (*e.g.*, the representations of the reference image, modification text, and matching tokens) can be modeled. Then the matching tokens can fully aggregate the related features from the multimodal query and the target image, respectively. 2) The length of the modification text varies in different samples, while Transformer is born to handle sequential data in variable lengths.

3.2.3 Query-Target Matching Modeling

Through the latent factor-oriented feature aggregation module, we have derived the Ψ_r and Ψ_t , which aggregate factor-related features from the multimodal query and the target image, respectively. The CIR task then boils down to making them close in the latent matching space. Towards this end, we first apply L2 normalization to each column of Ψ_r and Ψ_t . Let $\hat{\Psi}_r$ and $\hat{\Psi}_t$ denote the normalized query and target matrices, respectively. Thereafter, we resort to the batch-based classification loss [7], [10], which has shown convincing success in the task of CIR. The core of the batch-based classification loss is to ensure the target representation is the closest one to the corresponding query representation in a mini-batch, where other target images are treated as negative samples. Formally, we have,

$$\mathcal{L}_{\text{ranking}} = \frac{1}{B} \sum_{i=1}^B -\log \left\{ \frac{\exp \{s(\phi_{ri}, \phi_{ti}) / \tau\}}{\sum_{j=1}^B \exp \{s(\phi_{ri}, \phi_{tj}) / \tau\}} \right\}, \quad (11)$$

where $\phi_{ri} \in \mathbb{R}^{d'}$ and $\phi_{ti} \in \mathbb{R}^{d'}$ refer to the query representation and target representation of the i -th triplet sample in the mini-batch, which can be derived by reshaping $\hat{\Psi}_{ri}$ and $\hat{\Psi}_{ti}$ into a vector, respectively. $d' = D * U$. B is the batch size, $s(\cdot, \cdot)$ denotes the inner product, and τ is the temperature factor. Note that since Ψ_{ri} and Ψ_{ti} are first processed by L2 normalization, the inner product of ϕ_{ri} and ϕ_{ti} equals to summing the cosine similarities between each corresponding column of Ψ_{ri} and Ψ_{ti} . In other words, the inner product evaluates the matching degree between the multimodal query and the target image by jointly considering the U matching factors.

Notably, since there are no direct signals of the multi-faceted query-target matching factors to supervise the representation learning of matching tokens, the different matching tokens learned simply with the loss in Eqn. (11) may be homogenized [34]. Consequently, to ensure that different matching tokens can aggregate features from different aspects, we additionally introduce the factor-orthogonal regularization towards the Transformer output embeddings Ψ_r and Ψ_t . Formally, the factor-orthogonal regularization is written as follows,

$$\mathcal{L}_{\text{ortho}} = \frac{1}{B} \sum_{i=1}^B \left(\left\| \hat{\Psi}_{ri}^T \hat{\Psi}_{ri} - \mathbf{I} \right\|_F^2 + \left\| \hat{\Psi}_{ti}^T \hat{\Psi}_{ti} - \mathbf{I} \right\|_F^2 \right), \quad (12)$$

where $\mathbf{I} \in \mathbb{R}^{U \times U}$ is the identity matrix, and $\|\cdot\|_F$ refers to the Frobenius norm of matrix.

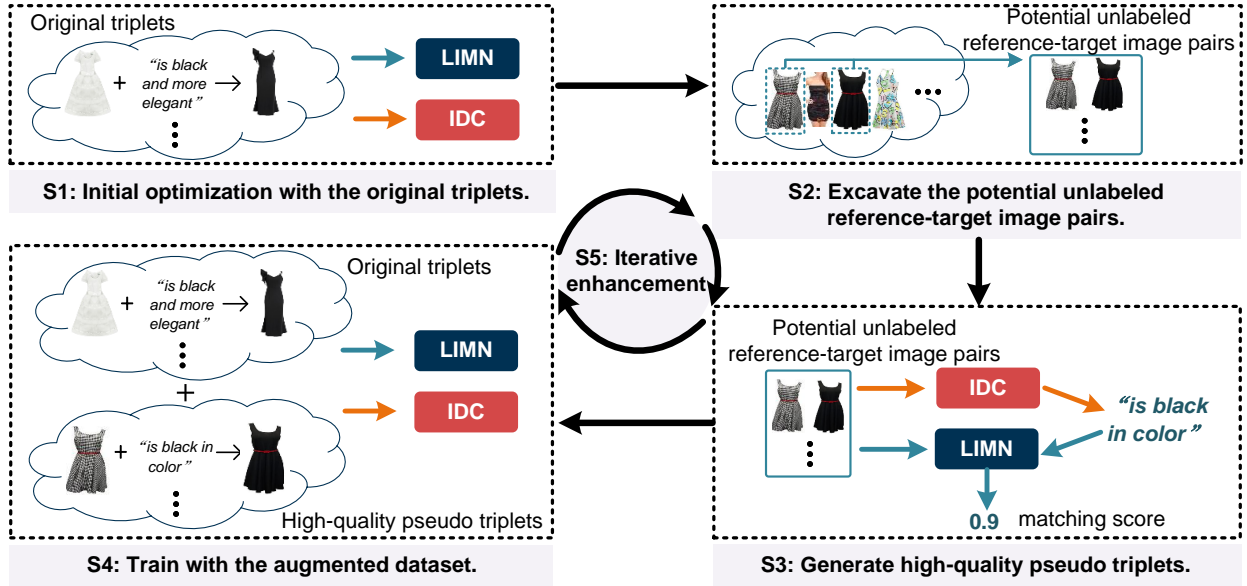


Fig. 3. The proposed iterative dual self-training paradigm for boosting the performance of LIMN and deriving LIMN+, which consists of five steps.

Ultimately, we have the following objective function for optimizing our LIMN,

$$\Theta^* = \arg \min_{\Theta} (\mathcal{L}_{ranking} + \lambda \mathcal{L}_{ortho}), \quad (13)$$

where Θ denotes the to-be-learned parameters in LIMN, and λ is the trade-off hyper-parameter. Once LIMN is well-trained, all the gallery images can be ranked by their cosine similarities with the input multimodal query according to Eqn. (11), and the CIR task gets solved.

3.3 Iterative Dual Self-Training Paradigm

Another major novelty of our work is that we resort to the self-training technique to fully exploit the unlabeled data, so as to alleviate the overfitting phenomenon caused by the limited size of training data. Self-training is a commonly used semi-supervised technique in the image classification field [35]–[37], which typically aims to first train a model with the labeled data, and then employ the well-trained model to derive pseudo labeled data by labeling the unlabeled data. Finally, both the labeled and pseudo labeled data are jointly utilized to train another model, which usually yields better performance than the model trained purely with the pre-labeled data.

To adapt the self-training strategy to the CIR task, we involve a highly correlated task to our CIR task, *i.e.*, image difference captioning (IDC for short) [20], [21], [38]–[41], which aims to generate a natural language-based text to describe the difference between the two relevant images. It is apparent that the dataset for the CIR task can be easily re-purposed for the IDC task, and vice versa. For example, each training triplet for CIR can be re-used for IDC, where the input is the image pair (x_r, x_t) , while the output is the corresponding modification text t_m . Therefore, we devise an iterative dual self-training paradigm that takes advantage of the duality between the two highly correlated tasks, to boost the performance in CIR. Specifically, in each iteration, we utilize a well-trained IDC model to generate extra pseudo

triplets for augmenting the training dataset of the CIR model and hence promoting its generalization ability. Meanwhile, to get rid of the noisy triplets, we employ the well-trained CIR model to evaluate the quality of the pseudo triplets generated by the IDC model.

Combing our context, we illustrate the devised iterative dual self-training paradigm in Figure 3, where the CIR model is instantiated with the proposed LIMN, while the IDC model not specified as any advanced IDC model is applicable. Notably, our proposed iterative dual self-training paradigm can be also applied to other CIR models to boost their performance. As can be seen from Figure 3, the iterative dual self-training paradigm can be summarized with five steps as follows.

- S1: Initial optimization with the original triplets.** Optimize the LIMN model and the IDC model based on the original training dataset, respectively. Let Θ'_* denote the parameters of the LIMN model and Φ'_* indicate the parameters of the IDC model.
- S2: Excavate the potential unlabeled reference-target image pairs.** Following the original reference-target image pair construction method of each dataset, we can excavate all the potential unlabeled reference-target image pairs from the training dataset \mathcal{T} , denoted as $\{(\hat{x}_r, \hat{x}_t)_j\}_{j=1}^M$. Note that different datasets differ in constructing image pairs, which will be detailed in Section 4.
- S3: Generate high-quality pseudo triplets.** Employ the well-trained IDC model to generate the modification text that describes the difference between the potential unlabeled reference-target image pairs, which is as follows,

$$\tilde{t}_m = \text{IDC} \left((\hat{x}_r, \hat{x}_t), \Phi'_* \right). \quad (14)$$

In this way, we can obtain the pseudo triplets $(\hat{x}_r, \tilde{t}_m, \hat{x}_t)$. To ensure the quality of pseudo triplets, we utilize the well-trained LIMN model to measure the

matching score between the multimodal query and the target image in each pseudo triplet, *i.e.*,

$$s = \text{LIMN} \left((\hat{x}_r, \tilde{t}_m, \hat{x}_t), \Phi'_* \right). \quad (15)$$

Thereafter, the pseudo triplets are sorted in descending order according to their corresponding matching scores s . The top κ pseudo triplets with high quality will be retained, and others will be removed.

S4: Train with the augmented dataset. The high-quality pseudo triplets and the original triplets are combined to re-train the LIMN model Θ''_* and the IDC model Φ''_* , respectively.

S5: Iterative enhancement. Repeat step2 - step4 until the performance of LIMN no longer increases, and it can be exercised during the inference stage.

For clarity, we denote the iterative dual self-training paradigm boosted LIMN as LIMN+.

4 EXPERIMENT

In this section, we first give the experimental settings and then detail the experiments conducted on three real-world datasets by answering the following research questions:

- **RQ1:** Do our models (LIMN and LIMN+) surpass state-of-the-art methods?
- **RQ2:** How does each component affect LIMN?
- **RQ3:** Does the devised iterative dual self-training paradigm boost the model performance?
- **RQ4:** How is the quantitative performance of LIMN+?

4.1 Experimental Settings

4.1.1 Datasets

There have been several public datasets in the domain of CIR. According to the modification text construction manner, the datasets can be classified into two groups: attribute-based datasets [7], [42], [43] and natural language-based datasets [44]–[46]. The modification text in the former group is synthesized by pre-specified templates, such as “replace A with B ”, which are not flexible and the application prospect is limited. In contrast, the modification text of datasets in the latter group is human-annotated, which is more flexible for users to express the modification demands. To evaluate our model, we chose three real-world natural language-based datasets: FashionIQ [44], Shoes [47], and Birds-to-Words [46]. The first two datasets belong to the fashion domain, and the third one focuses on the topic of birds. They are close to real-world application scenarios.

FashionIQ [44] is an interactive fashion retrieval dataset. The fashion items within belong to three categories: Dresses, Tops&Tees, and Shirts. Following [8], [10], [16], $\sim 46\text{K}$ images and $\sim 15\text{K}$ images are used for training and testing, respectively. Finally, there are 18K triplets for training and $\sim 6\text{K}$ for testing.

Shoes [47] is originally created for the attribute discovery task by [45], and is then developed with relative caption annotations for the dialog-based interactive retrieval task [47]. Following [8], [10], [16], 10K images are used for training and $\sim 4.6\text{K}$ images for testing, in which $\sim 9\text{K}$ triplets and $\sim 1.7\text{K}$ triplets are constructed, respectively.

Birds-to-Words [46] is a dataset originally introduced for the image difference captioning task, where the image pairs are tagged with descriptions of fine-grained differences. Following [15], we applied it to the CIR task. There are $\sim 2.8\text{K}$ images in the training set and $\sim 0.7\text{K}$ images in the testing set, where $\sim 2.7\text{K}$ training image pairs and $\sim 0.6\text{K}$ testing image pairs are constructed. Each image pair is tagged with 4.8 descriptions on average, resulting in $\sim 12\text{K}$ triplets and $\sim 3\text{K}$ triplets for training and testing, respectively.

4.1.2 Implementation Details

For the LIMN model, both the dimensions of visual and textual representations are set to 1,024. The parameter-shared Transformer for processing the multimodal query and the target image is set to 2 layers and 4 heads for the FashionIQ and the Birds-to-Words dataset, while 1 layer and 8 heads for the Shoes dataset. The temperature factor in Eqn. (11) is set to 10. We trained LIMN by Adam optimizer [48] with the learning rate of 0.0001, which multiplies 0.1 at the 10-th epoch. We empirically set the batch size as 32. The number of matching tokens U is set as 15, 25, and 5 for FashionIQ, Shoes, and Birds-to-Words through hyperparameter tuning, respectively. Regarding the trade-off hyper-parameter λ , we conducted grid search among [0.01, 0.1, 0.5, 1] for the three datasets, and finally set $\lambda = 0.1, 1.0, \text{ and } 1.0$ for FashionIQ, Shoes, and Birds-to-Words, respectively. For a fair comparison, we utilized the same evaluation metric, *i.e.*, recall at rank k ($R@k$), as previous efforts [8], [10], [15], [16] to measure the image retrieval performance.

Pertaining to the iterative dual self-training paradigm, we directly utilized the off-the-shelf DUDA [38] as the IDC model². We trained DUDA by Adam optimizer with a fixed learning rate of 0.0001, where the batch size is set to 32. We resorted to the widely-used BLEU-1 [49] and ROUGE-L [50] metrics to evaluate the quality of the generated pseudo triplets. The numbers of the retained pseudo triplets κ are empirically set to 6,000 for each category in FashionIQ, 9,000 for Shoes, and 10,000 for Birds-to-Words, respectively, which are comparable to the size of the original training set of the three datasets.

4.1.3 Potential Unlabeled Reference-Target Image Pairs Construction

According to the step2 of our iterative dual self-training paradigm, we need to find the potential unlabeled reference-target image pairs. To ensure the distribution of pseudo triplets as consistent as possible with that of the original dataset, we attempted to excavate the potential unlabeled reference-target image pairs in the same manner as the original image pair construction of each dataset as follows.

1) For the FashionIQ dataset, following [44], for each training image, we first computed the TF-IDF score of each word in its corresponding fashion item title. We then paired each training image with another training image that achieves the maximum value of the summation over the TF-IDF scores on all overlapping words between the two

² Any other model architecture applicable to the IDC task is acceptable. As this is not the focus of this work, we directly choose the off-the-shelf DUDA model.

TABLE 1

Performance comparison on FashionIQ with respect to $R@k(\%)$. The best results over baselines are underlined, while the overall best results are in boldface. The last row indicates the performance improvements by LIMN+ over the best baseline. The utilized visual and textual features of each method are illustrated correspondingly.

Method	Visual feature	Textual feature	FashionIQ							
			Dress		Shirt		Tops&Tees		Avg	
			R@10	R@50	R@10	R@50	R@10	R@50	R@10	R@50
TIRG [7]	Global	Sentence-level	14.87	34.66	18.26	37.89	19.08	39.62	17.40	37.39
ComposeAE [11]			14.03	35.10	13.88	34.59	15.80	39.26	19.89	36.31
ARTEMIS [9]			27.16	52.40	21.78	43.64	29.20	54.83	26.05	50.29
VAL [8]	Local	Sentence-level	21.12	42.19	21.03	43.44	25.64	49.49	22.60	45.04
CosMo [13]			25.64	50.30	24.90	49.18	29.21	57.46	26.58	52.31
DATIR [14]			21.90	43.80	21.90	43.70	27.20	51.60	23.70	46.40
SAC [15]			26.52	51.01	28.02	51.86	32.70	61.23	29.08	54.70
HFFCA [51]	Local and Global	Word- and Sentence-level	26.20	51.20	22.40	46.00	29.70	56.40	26.10	51.20
DCNet [16]			28.95	56.07	23.95	47.30	30.44	58.29	27.78	53.89
CLVC-Net [10]			29.85	56.47	28.75	54.76	33.50	64.00	30.70	58.41
EER [52]			30.02	55.44	25.32	49.87	33.20	60.34	29.51	55.22
CRR [17]	Local	Word-level	<u>30.41</u>	<u>57.11</u>	<u>30.73</u>	<u>58.02</u>	<u>33.67</u>	<u>64.48</u>	<u>31.60</u>	<u>59.87</u>
LIMN	Local and Global	Word- and Sentence-level	34.85	60.68	33.56	59.18	40.49	66.75	36.30	62.20
LIMN+			35.60	62.37	34.69	59.81	40.64	68.33	36.98	63.50
Gains(%)			↑ 17.07	↑ 9.21	↑ 12.89	↑ 3.09	↑ 20.70	↑ 5.97	↑ 17.03	↑ 6.06

items' titles. Finally, we obtained $\sim 30K$ potential unlabeled reference-target image pairs for the FashionIQ dataset, of which 7,741 belong to the category of Dress, 9,925 to the Tops&Tees, and 12,062 to the Shirts.

2) Regarding the Shoes dataset, as [47] did not release the details for constructing the reference-target image pairs, we proposed a statistic-based strategy to find the potential unlabeled reference-target image pairs. In particular, we first computed the similarity score of each reference-target image pair in the training set with our pre-trained LIMN. It shows that the mean and variance of the similarity scores in the whole training set are 0.9703 and 0.0153, respectively. Accordingly, we randomly selected two images, and retained them as long as their similarity score falls in the range of $[0.9703 - 0.0153, 0.9703 + 0.0153]$. Ultimately, we obtained 20,000 potential unlabeled reference-target image pairs.

3) As for the Birds-to-Words dataset, we followed the image pairs construction manner of the original dataset [46] that utilizes both the taxonomy and visual similarity measures. Specifically, for the taxonomy similarity measure, we first crawled the taxonomy information (such as species, genus, and family) of each training image from iNaturalist³. Then for each training image, we sampled another two images as two reference images from the same taxonomy levels to derive two reference-target image pairs. In this manner, we obtained 6,840 potential unlabeled reference-target image pairs. As for the visual similarity measure, for each image in the training set, we resorted to the pre-trained LIMN to select the two most similar images as two reference images, resulting in 5,646 reference-target image pairs in total. Ultimately, we obtained 12,496 potential unlabeled reference-target image pairs.

4.2 Performance Comparison (RQ1)

To justify the effectiveness of our proposal, we chose the following baselines for comparison: TIRG [7], VAL [8], ComposeAE [11], SAC [15], CosMo [13], HFFCA [51], DATIR [14], DCNet [16], CLVC-Net [10], ARTEMIS [9],

3. <https://www.inaturalist.org>.

TABLE 2

Performance comparison on Shoes and Birds-to-Words datasets with respect to $R@k(\%)$. Cells in colors indicate results obtained by re-running the released codes on the desired dataset. The missing results are because the source codes are not available yet. The best baseline results are underlined, while the overall best results are in boldface. The last row is the performance improvements by LIMN+ over the best baseline results.

Method	Shoes		Birds-to-Words	
	R@10	R@50	R@10	R@50
TIRG [7]	45.45	69.39	15.80	38.65
ComposeAE [11]	19.36	47.58	10.66	34.84
ARTEMIS [9]	53.11	79.31	25.94	45.93
VAL [8]	49.12	73.53	23.90	41.51
CosMo [13]	48.36	75.64	23.07	43.04
DATIR [14]	51.10	75.60	-	-
SAC [15]	51.73	77.28	19.56	45.24
HFFCA [51]	50.95	77.24	-	-
DCNet [16]	53.82	79.33	-	-
CLVC-Net [10]	54.39	79.47	28.10	54.32
EER [52]	56.02	79.94	-	-
CRR [17]	56.38	79.92	-	-
LIMN	56.90	80.01	35.03	60.58
LIMN+	57.30	82.17	40.34	66.18
Gains(%)	↑ 1.63	↑ 2.79	↑ 43.56	↑ 21.83

CRR [17], and EER [52]. Tables 1 and 2 summarize the performance comparison among different methods on the three datasets. From these tables, we have the following observations. 1) LIMN+ consistently outperforms all the baseline methods over three datasets by a large margin. Notably, LIMN+ gains 17.03% and 40.34% improvements on FashionIQ-Avg and Birds-to-Words over the best baseline with respect to $R@10$, respectively, and 2.79% improvement on Shoes regarding $R@50$. This confirms the superiority of our LIMN+ that utilizes the multiple matching tokens to capture the multi-faceted query-target matching factors, as well as employs the iterative dual self-training paradigm to relieve the overfitting problem caused by the limited dataset size. 2) Equipped with the latent matching factor modeling, LIMN surpasses all the baseline methods on FashionIQ and Birds-to-Words datasets significantly, and delivers com-

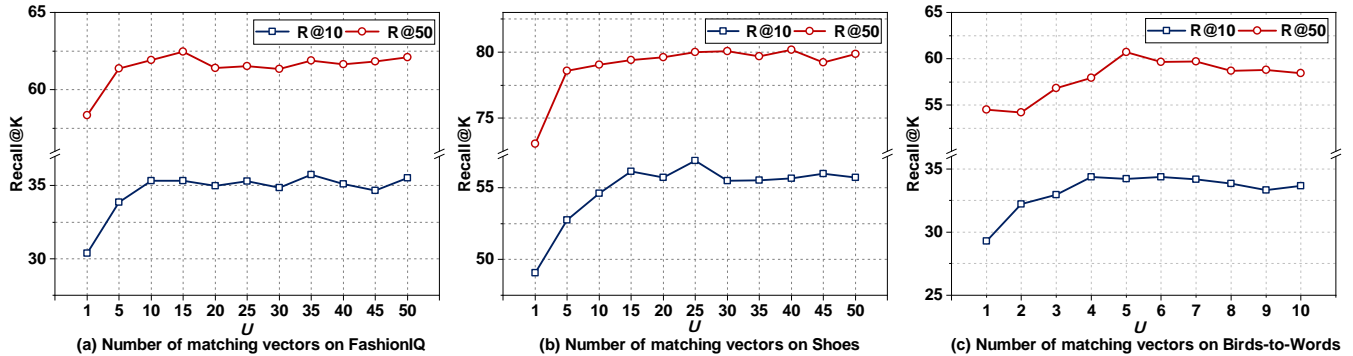
Fig. 4. Influence of the number of matching tokens U on (a) FashionIQ, (b) Shoes, and (c) Birds-to-Words.

TABLE 3

Performance comparison among our model derivations on three datasets with respect to $R@k(\%)$. The results on FashionIQ are the average results of three categories.

Method	FashionIQ-Avg		Shoes		Birds-to-Words	
	R@10	R@50	R@10	R@50	R@10	R@50
w/ OneFactor	31.08	57.46	49.06	73.08	31.44	57.06
w/ Avepool	33.09	60.22	52.81	76.38	31.66	59.09
w/o Ortho	34.21	61.43	55.20	79.22	34.30	58.39
w/o Global	34.67	61.51	53.61	78.65	23.97	43.64
w/o Local	25.33	50.86	48.15	73.76	30.11	51.68
LIMN	36.30	62.20	56.90	80.01	35.03	60.58

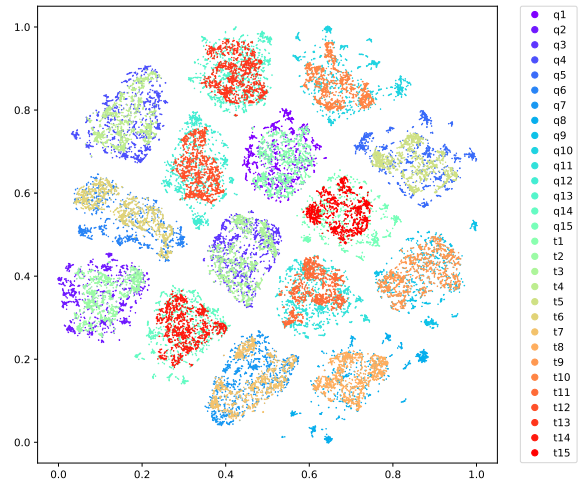
parable results on Shoes dataset. This observation reflects the powerful capability of our LIMN for the CIR tasks. 3) With the iterative dual self-training paradigm, LIMN+ consistently improves the performance of LIMN on three datasets, which verifies the effectiveness of introducing the self-training technique to the CIR task.

4.3 Ablation Study (RQ2)

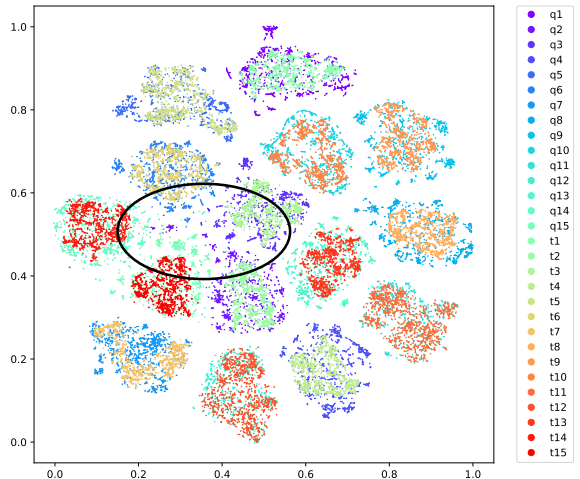
To verify the importance of each component in LIMN, we compared LIMN with its following derivatives.

- **w/ OneFactor:** To investigate the effect of introducing the multiple matching tokens, we used only one matching token in the latent factor-oriented feature aggregation module by setting $U = 1$.
- **w/ Avepool:** To study the role of summing the cosine similarities on all matching factors in evaluating the matching degree between the multimodal query and target image (see Eqn. (11)), we exerted the average pooling operation to the representations of multiple matching tokens (*i.e.*, Φ_r and Φ_t) by columns, and based on the resulted vectors to compute the cosine similarity.
- **w/o Ortho:** To study the effect of the factor-orthogonal regularization, we removed this constraint by setting $\lambda = 0$ in Eqn. (12).
- **w/o Global:** To check the importance of utilizing both global visual and textual features, we removed the global visual feature E_r^G from Eqn. (4) and the sentence-level representation E_m^S from Eqn. (8).
- **w/o Local:** Similarly, we removed the local visual feature E_r^L from Eqn. (4) and the word-level representation E_m^W from Eqn. (8).

Table 3 shows the ablation results of LIMN on three datasets. From this table, we gained the following obser-



(a) LIMN on FashionIQ-Dress



(b) w/o Ortho on FashionIQ-Dress

Fig. 5. Visualization of the learned representations of multiple matching tokens by our LIMN and its derivative w/o Ortho for the testing samples in FashionIQ-Dress. Different colors indicate different matching tokens. “q k ” and “t k ” in legends denote the k -th matching token for the multimodal query and the target image, respectively.

variations. 1) w/ OneFactor performs worse than our LIMN, which proves the necessity of utilizing multiple matching tokens to model the multi-faceted query-target matching factors. 2) w/ Avepool also shows inferior results compared

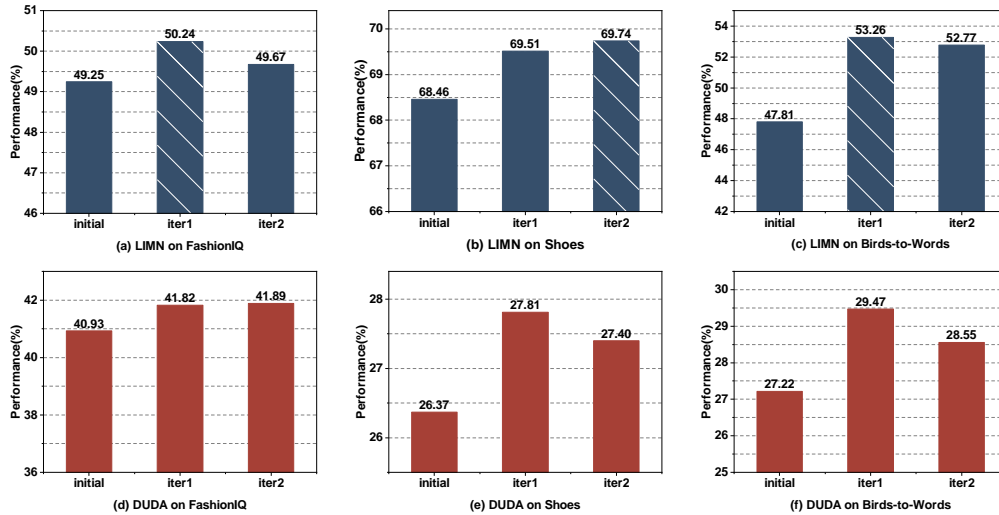


Fig. 6. The iterative performance of our CIR model LIMN and the IDC model DUDA under the iterative dual self-training paradigm on FashionIQ, Shoes, and Birds-to-Words datasets. The performance of CIR is the average of $R@k$, and that of IDC is the average between BLEU-1 and ROUGE-L. The three bars in each plot refer to the initial performance of the original model, performance by the 1 self-training iteration, and performance by 2 self-training iterations, respectively. The bars with white slashes indicate the optimal performance reported in this work.

to LIMN. This indicates that when utilizing the multiple matching tokens to evaluate the query-target matching, the late-fusion manner LIMN used (*i.e.*, summing the similarities of each matching token between the multimodal query and the target image by the inner product) performs better than the early-fusion manner w/ Avepool used (*i.e.*, first averaging the representations of the multiple matching tokens, and then performing the query-target matching). 3) LIMN surpasses w/o Ortho, indicating that the designed factor-orthogonal regularization is indeed helpful to guarantee independence and reduce redundancy among different matching tokens. 4) Both w/o Global and w/o Local are inferior to LIMN, which validates that it is essential to incorporate the multi-grained visual and textual features in CIR.

To provide more insight into the effect of multiple matching tokens in LIMN, we illustrated the performance of our LIMN with respect to different numbers of matching tokens on three datasets in Figure 4. Notably, the range of the number of matching tokens explored for each dataset is set according to the corresponding optimal value of U . From Figure 4, we observed that as the number of matching tokens increases, the performance of LIMN on three datasets first rises and then tends to be stable. The observed results are reasonable since more matching tokens can cover more matching factors, and the retrieval performance will be better. Nevertheless, too many matching tokens will not bring additional performance improvement. This may be due to the fact that the number of useful matching factors in real-world application scenarios is limited and thus introducing more to-be-learned matching tokens is redundant and can lead to overfitting.

Furthermore, to intuitively reflect the strength of the factor-orthogonal regularization, using the tool of t-SNE [53], [54], we visualized the learned representations of multiple matching tokens by our LIMN and its derivative w/o Ortho for the testing samples in FashionIQ-Dress in Figure 5. Different color indicates different matching to-

kens, where we also differentiated the colors for the same matching token derived from different sources (*i.e.*, either the multimodal query or the target image). According to our experiment setting, for the FashionIQ dataset, the number of matching tokens is set to 15. Therefore, there are 30 different colors in each plot. From this figure, we have the following observations. 1) For both methods, the distributions of the matching tokens for the multimodal query and the target image are homogeneous, which is reasonable as we make the Transformers that process the multimodal query and the target image sharing the same parameters. 2) For both methods, points corresponding to the same matching token are clustered together, while those of different matching tokens are grouped into different clusters. This suggests that the learned different matching tokens tend to capture different matching factors. 3) Without the factor-orthogonal regularization, the clustering effect of w/o Ortho is worse than LIMN, where the black circle in Figure 5 (b) denotes that some representations of different tokens are mixed up and cannot be well distinguished. This phenomenon validates the effect of our proposed factor-orthogonal regularization in ensuring independency among the multiple matching factors.

4.4 Iterative Dual Self-training Paradigm (RQ3)

In this subsection, to thoroughly explore the effectiveness of the proposed iterative dual self-training paradigm, we conducted experiments to investigate the self-training iterative performance of the CIR and IDC models, as well as the generalization ability of the iterative dual self-training paradigm towards CIR.

4.4.1 Self-training Iterative Performance

To gain a more comprehensive understanding of our proposed iterative dual self-training paradigm, we investigated the performance of our LIMN model and the IDC model,

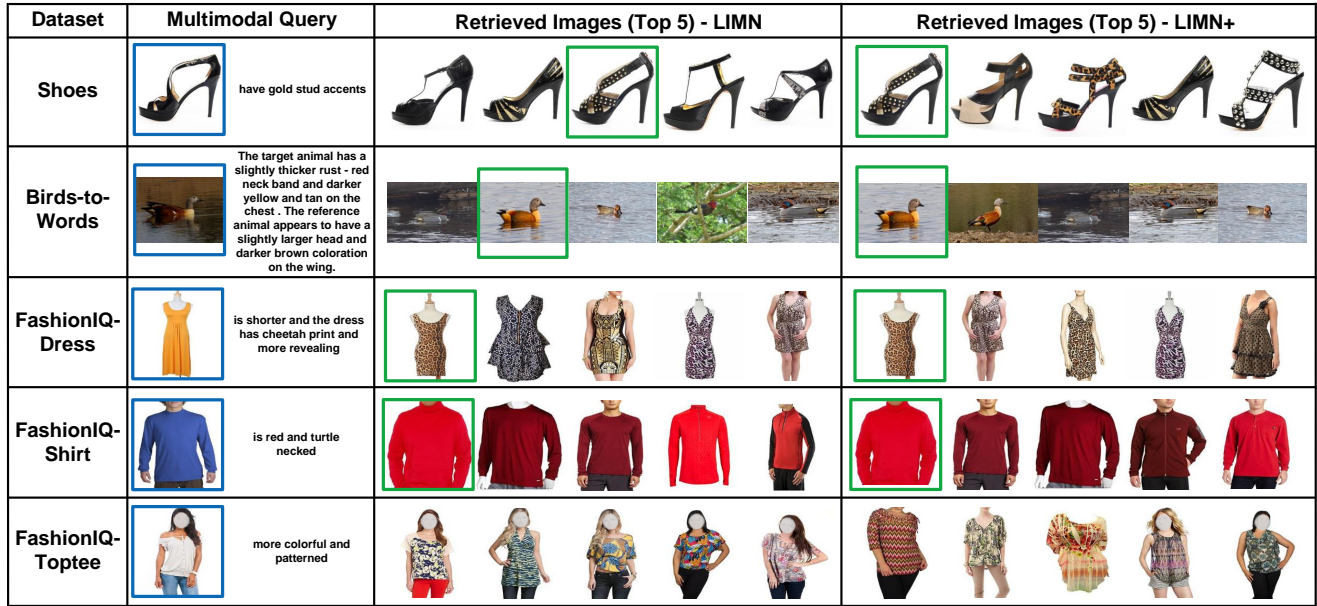


Fig. 7. Illustration of several CIR results obtained by our LIMN and LIMN+ on three datasets.

i.e., DUDA, in each iteration under the iterative dual self-training paradigm on three datasets. As illustrated in Figure 6, compared to the initial performance, the iterative dual self-training paradigm consistently boosts the image retrieval performance of LIMN and the image difference captioning performance of DUDA on three datasets. This confirms that the advantage of our proposed iterative dual self-training paradigm in fully utilizing the potential unlabeled reference-target image pairs and relieving the setback of the limited training data. Moreover, as can be seen, in most cases, the performance improvement by only one self-training iteration is significant, which suggests the high efficiency of our iterative dual self-training paradigm.

4.4.2 Generalization towards CIR

TABLE 4
Self-training boosted CLVC-Net performance. The results on FashionIQ are the average result of three categories.

Method	FashionIQ-Avg		Shoes		Birds-to-Words	
	R@10	R@50	R@10	R@50	R@10	R@50
CLVC-Net	30.70	58.41	54.39	79.47	28.10	54.32
CLVC-Net+	31.55	60.24	55.07	80.12	39.29	66.01
Gains(%)	↑ 2.77	↑ 3.13	↑ 1.25	↑ 0.82	↑ 39.82	↑ 21.52

To study the generality of the devised iterative dual self-training paradigm for the CIR task, we also selected the public CLVC-Net [10] model as the CIR model in our self-training paradigm. We named the self-training boosted CLVC-Net as CLVC-Net+. The experimental settings are identical to LIMN+. Table 4 shows the performance of CLVC-Net and CLVC-Net+ on the three datasets. As can be seen, CLVC-Net+ consistently outperforms the original CLVC-Net. Particularly, the performance gains much more on the Birds-to-words dataset, which is 39.82% and 21.52% over R@10 and R@50, respectively. This may be due to the fact that the data is more scarce and the overfitting phenomenon is relatively more serious in this dataset, as

compared to FashionIQ and Shoes datasets. Overall, the results reflect the generalization ability of our proposed iterative dual self-training paradigm for the task of CIR.

4.5 Case Study (RQ4)

Figure 7 illustrates several CIR results obtained by our LIMN and LIMN+ on three datasets. We reported the top 5 retrieved images for the limited space. We utilized blue and green boxes to indicate the reference and target images, respectively. As shown in Figure 7(a), we observed that LIMN fails to rank the target image in the first place, while LIMN+ successfully raises the target image from the third place to the first place. The reason is that the desired item feature “stud” is rare (39 related samples) in the original training set. Benefiting from more training samples (8 augmented related samples), the self-training boosted LIMN+ model can perform better on reasoning the rare features, thereby gaining better image retrieval performance. This is also reflected in the case of Figure 7(b) sampled from the Birds-to-Words dataset, where LIMN ranks the target image at the second place, while LIMN+ tops the target image. Regarding cases in Figure 7(c) and Figure 7(d), the target images are ranked at the first place by both LIMN and LIMN+, yet we noticed that the top 5 images retrieved by LIMN+ meet the multimodal query better than those retrieved by LIMN. For example, in the case of Figure 7(c), the dresses in the second-ranked image and the third-ranked image retrieved by LIMN are not with cheetah print, while those by LIMN+ has the desired print. This suggests the superiority of our designed iterative dual self-training paradigm in CIR again. Meanwhile, we also noticed some failing examples (see Figure 7(e)) of our models, where the target image is not retrieved within the top 5 places by both models. Looking into this case, we observed that all the top 5 retrieved shirts of our models meet the requirement of the multimodal query. We attributed this phenomenon to the flaws of the dataset itself, where the false-negative

images are not labeled as target images [9]. Overall, these observations show our models' effectiveness and practical value, and validate the benefit of introducing the iterative dual self-training paradigm.

5 CONCLUSION AND FUTURE WORK

In this work, we first present a novel multi-faceted Matching Network (LIMN) to explore the latent matching factors affecting the matching evaluation between the multimodal query and the target image. Moreover, we design an iterative dual self-training paradigm to take full use of the potential unlabeled reference-target image pairs in the dataset, so as to relieve the problem of limited data size. Extensive experiments are conducted on three natural language-based CIR datasets, and the results prove the effectiveness of our proposed method. As expected, we observed that by considering the multi-faceted query-target matching factors, the designed LIMN method shows cutting-edge performance compared to existing efforts. Additionally, the proposed iterative dual self-training paradigm can further boost the image retrieval performance by excavating the value of the potential unlabeled reference-target image pairs. Overall, this work provides a novel approach along with complete experiments, which advances the research in the CIR community.

Currently, we mainly utilized the IDC method as an assistant to improve the performance of the CIR method. To take it further, we will extend our method to solve the CIR task and the IDC task simultaneously within a unified framework, as the two tasks are highly correlated. In addition, we can adjust the proposed method to solve the multi-turn interactive image retrieval task, which is essential in multimodal dialogue systems.

ACKNOWLEDGMENTS

REFERENCES

- [1] R. Datta, D. Joshi, J. Li, and J. Z. Wang, "Image retrieval: Ideas, influences, and trends of the new age," *ACM Computing Surveys*, vol. 40, no. 2, pp. 5:1–5:60, 2008.
- [2] C. Fu, X. Wu, Y. Hu, H. Huang, and R. He, "Dvg-face: Dual variational generation for heterogeneous face recognition," *IEEE Transactions on Pattern Analysis and Machine Intelligence*, vol. 44, no. 6, pp. 2938–2952, 2022.
- [3] C. Zhang, H. Li, C. Chen, Y. Qian, and X. Zhou, "Enhanced group sparse regularized nonconvex regression for face recognition," *IEEE Transactions on Pattern Analysis and Machine Intelligence*, vol. 44, no. 5, pp. 2438–2452, 2022.
- [4] X. Yang, X. Song, X. Han, H. Wen, J. Nie, and L. Nie, "Generative attribute manipulation scheme for flexible fashion search," in *Proceedings of the International ACM SIGIR conference on research and development in Information Retrieval*. ACM, 2020, pp. 941–950.
- [5] J. Li, S. Zhang, Q. Tian, M. Wang, and W. Gao, "Pose-guided representation learning for person re-identification," *IEEE Transactions on Pattern Analysis and Machine Intelligence*, vol. 44, no. 2, pp. 622–635, 2022.
- [6] M. Liu, L. Qu, L. Nie, M. Liu, L. Duan, and B. Chen, "Iterative local-global collaboration learning towards one-shot video person re-identification," *IEEE Transactions on Image Processing*, vol. 29, pp. 9360–9372, 2020.
- [7] N. Vo, L. Jiang, C. Sun, K. Murphy, L. Li, L. Fei-Fei, and J. Hays, "Composing text and image for image retrieval - an empirical odyssey," in *Proceedings of the IEEE Conference on Computer Vision and Pattern Recognition*. IEEE, 2019, pp. 6439–6448.
- [8] Y. Chen, S. Gong, and L. Bazzani, "Image search with text feedback by visiolinguistic attention learning," in *Proceedings of the IEEE Conference on Computer Vision and Pattern Recognition*. IEEE, 2020, pp. 2998–3008.
- [9] G. Delmas, R. S. Rezende, G. Csurka, and D. Larlus, "Artemis: Attention-based retrieval with text-explicit matching and implicit similarity," in *Proceedings of the International Conference on Learning Representations*. OpenReview.net, 2022, pp. 1–12.
- [10] H. Wen, X. Song, X. Yang, Y. Zhan, and L. Nie, "Comprehensive linguistic-visual composition network for image retrieval," in *Proceedings of the International ACM SIGIR Conference on Research and Development in Information Retrieval*. ACM, 2021, pp. 1369–1378.
- [11] M. U. Anwaar, E. Labintcev, and M. Kleinstueber, "Compositional learning of image-text query for image retrieval," in *Proceedings of the IEEE Winter Conference on Applications of Computer Vision*. IEEE, 2021, pp. 1139–1148.
- [12] M. Hosseinzadeh and Y. Wang, "Composed query image retrieval using locally bounded features," in *Proceedings of the IEEE Conference on Computer Vision and Pattern Recognition*. IEEE, 2020, pp. 3593–3602.
- [13] S. Lee, D. Kim, and B. Han, "Cosmo: Content-style modulation for image retrieval with text feedback," in *Proceedings of the IEEE Conference on Computer Vision and Pattern Recognition*. IEEE, 2021, pp. 802–812.
- [14] C. Gu, J. Bu, Z. Zhang, Z. Yu, D. Ma, and W. Wang, "Image search with text feedback by deep hierarchical attention mutual information maximization," in *Proceedings of the International ACM Conference on Multimedia*. ACM, 2021, pp. 4600–4609.
- [15] S. Jandial, P. Badjatiya, P. Chawla, A. Chopra, M. Sarkar, and B. Krishnamurthy, "SAC: semantic attention composition for text-conditioned image retrieval," in *Proceedings of the IEEE Winter Conference on Applications of Computer Vision*. IEEE, 2022, pp. 597–606.
- [16] J. Kim, Y. Yu, H. Kim, and G. Kim, "Dual compositional learning in interactive image retrieval," in *Proceedings of the AAAI Conference on Artificial Intelligence*. AAAI, 2021, pp. 1771–1779.
- [17] F. Zhang, M. Yan, J. Zhang, and C. Xu, "Comprehensive relationship reasoning for composed query based image retrieval," in *Proceedings of the International ACM Conference on Multimedia*. ACM, 2022, pp. 4655–4664.
- [18] F. Zhang, M. Xu, Q. Mao, and C. Xu, "Joint attribute manipulation and modality alignment learning for composing text and image to image retrieval," in *Proceedings of the International ACM Conference on Multimedia*. ACM, 2020, pp. 3367–3376.
- [19] A. Vaswani, N. Shazeer, N. Parmar, J. Uszkoreit, L. Jones, A. N. Gomez, L. Kaiser, and I. Polosukhin, "Attention is all you need," in *Proceedings of the Advances in Neural Information Processing Systems*. MIT Press, 2017, pp. 5998–6008.
- [20] H. Jhamtani and T. Berg-Kirkpatrick, "Learning to describe differences between pairs of similar images," in *Proceedings of the Conference on Empirical Methods in Natural Language Processing*. Association for Computational Linguistics, 2018, pp. 4024–4034.
- [21] M. Hosseinzadeh and Y. Wang, "Image change captioning by learning from an auxiliary task," in *Proceedings of the IEEE Conference on Computer Vision and Pattern Recognition*. IEEE, 2021, pp. 2725–2734.
- [22] S. C. Fralick, "Learning to recognize patterns without a teacher," *IEEE Transactions on Information Theory*, vol. 13, no. 1, pp. 57–64, 1967.
- [23] Q. Xie, M. Luong, E. H. Hovy, and Q. V. Le, "Self-training with noisy student improves imagenet classification," in *Proceedings of the IEEE Conference on Computer Vision and Pattern Recognition*. IEEE, 2020, pp. 10 684–10 695.
- [24] Z. Ye, Y. Geng, J. Chen, J. Chen, X. Xu, S. Zheng, F. Wang, J. Zhang, and H. Chen, "Zero-shot text classification via reinforced self-training," in *Proceedings of the Annual Meeting of the Association for Computational Linguistics*. Association for Computational Linguistics, 2020, pp. 3014–3024.
- [25] Q. Yang, X. Wei, B. Wang, X. Hua, and L. Zhang, "Interactive self-training with mean teachers for semi-supervised object detection," in *Proceedings of the IEEE Conference on Computer Vision and Pattern Recognition*. IEEE, 2021, pp. 5941–5950.
- [26] J. Deng, W. Dong, R. Socher, L. Li, K. Li, and L. Fei-Fei, "Imagenet: A large-scale hierarchical image database," in *Proceedings of the IEEE Conference on Computer Vision and Pattern Recognition*. IEEE Computer Society, 2009, pp. 248–255.
- [27] K. He, X. Zhang, S. Ren, and J. Sun, "Deep residual learning for image recognition," in *Proceedings of the IEEE Conference on Computer Vision and Pattern Recognition*. IEEE, 2016, pp. 770–778.
- [28] G. Zhang, S. Wei, H. Pang, and Y. Zhao, "Heterogeneous feature fusion and cross-modal alignment for composed image retrieval,"

- in *Proceedings of the International ACM Conference on Multimedia*. ACM, 2021, pp. 5353–5362.
- [29] M. Yang, D. He, M. Fan, B. Shi, X. Xue, F. Li, E. Ding, and J. Huang, “DOLG: single-stage image retrieval with deep orthogonal fusion of local and global features,” in *Proceedings of the IEEE International Conference on Computer Vision*. IEEE, 2021, pp. 11 752–11 761.
- [30] J. Lin, R. Men, A. Yang, C. Zhou, Y. Zhang, P. Wang, J. Zhou, J. Tang, and H. Yang, “M6: multi-modality-to-multi-modality multitask mega-transformer for unified pretraining,” in *Proceedings of the International ACM SIGKDD Conference on Knowledge Discovery and Data Mining*. ACM, 2021, pp. 3251–3261.
- [31] F. Radenovic, G. Tolia, and O. Chum, “Fine-tuning CNN image retrieval with no human annotation,” *IEEE Transactions on Pattern Analysis and Machine Intelligence*, vol. 41, no. 7, pp. 1655–1668, 2019.
- [32] S. Hochreiter and J. Schmidhuber, “Long short-term memory,” *Neural Computation*, vol. 9, no. 8, pp. 1735–1780, 1997.
- [33] M. A. Islam, M. Kowal, S. Jia, K. G. Derpanis, and N. D. B. Bruce, “Global pooling, more than meets the eye: Position information is encoded channel-wise in cnns,” in *Proceedings of the IEEE International Conference on Computer Vision*. IEEE, 2021, pp. 773–781.
- [34] X. Wang, H. Jin, A. Zhang, X. He, T. Xu, and T. Chua, “Disentangled graph collaborative filtering,” in *Proceedings of the International ACM SIGIR Conference on Research and Development in Information Retrieval*. ACM, 2020, pp. 1001–1010.
- [35] Q. Xie, M. Luong, E. H. Hovy, and Q. V. Le, “Self-training with noisy student improves imagenet classification,” in *Proceedings of the IEEE Conference on Computer Vision and Pattern Recognition*. IEEE, 2020, pp. 10 684–10 695.
- [36] C. Wei, K. Sohn, C. Mellina, A. L. Yuille, and F. Yang, “Crest: A class-rebalancing self-training framework for imbalanced semi-supervised learning,” in *Proceedings of the IEEE Conference on Computer Vision and Pattern Recognition*. IEEE, 2021, pp. 10 857–10 866.
- [37] Y. Zou, Z. Yu, X. Liu, B. V. K. V. Kumar, and J. Wang, “Confidence regularized self-training,” in *Proceedings of the IEEE International Conference on Computer Vision*. IEEE, 2019, pp. 5981–5990.
- [38] D. H. Park, T. Darrell, and A. Rohrbach, “Robust change captioning,” in *Proceedings of the IEEE International Conference on Computer Vision*. IEEE, 2019, pp. 4623–4632.
- [39] H. Tan, F. Dernoncourt, Z. Lin, T. Bui, and M. Bansal, “Expressing visual relationships via language,” in *Proceedings of the Conference of the Association for Computational Linguistics*. Association for Computational Linguistics, 2019, pp. 1873–1883.
- [40] M. Forbes, C. Kaeser-Chen, P. Sharma, and S. J. Belongie, “Neural naturalist: Generating fine-grained image comparisons,” in *Proceedings of the Conference on Empirical Methods in Natural Language Processing and the International Joint Conference on Natural Language Processing*. Association for Computational Linguistics, 2019, pp. 708–717.
- [41] Z. Fei, “Actor-critic sequence generation for relative difference captioning,” in *Proceedings of the International Conference on Multimedia Retrieval*. ACM, 2020, pp. 100–107.
- [42] X. Han, Z. Wu, P. X. Huang, X. Zhang, M. Zhu, Y. Li, Y. Zhao, and L. S. Davis, “Automatic spatially-aware fashion concept discovery,” in *Proceedings of the IEEE International Conference on Computer Vision*. IEEE, 2017, pp. 1472–1480.
- [43] P. Isola, J. J. Lim, and E. H. Adelson, “Discovering states and transformations in image collections,” in *Proceedings of the IEEE Conference on Computer Vision and Pattern Recognition*. IEEE, 2015, pp. 1383–1391.
- [44] H. Wu, Y. Gao, X. Guo, Z. Al-Halah, S. Rennie, K. Grauman, and R. Feris, “Fashion IQ: A new dataset towards retrieving images by natural language feedback,” in *Proceedings of the IEEE Conference on Computer Vision and Pattern Recognition*. IEEE, 2021, pp. 11 307–11 317.
- [45] T. L. Berg, A. C. Berg, and J. Shih, “Automatic attribute discovery and characterization from noisy web data,” in *Proceedings of the European Conference on Computer Vision*. Springer, 2010, pp. 663–676.
- [46] M. Forbes, C. Kaeser-Chen, P. Sharma, and S. J. Belongie, “Neural naturalist: Generating fine-grained image comparisons,” in *Proceedings of the Conference on Empirical Methods in Natural Language Processing*. Association for Computational Linguistics, 2019, pp. 708–717.
- [47] X. Guo, H. Wu, Y. Cheng, S. Rennie, G. Tesauro, and R. S. Feris, “Dialog-based interactive image retrieval,” in *Proceedings of the Conference on Neural Information Processing Systems*. MIT Press, 2018, pp. 676–686.
- [48] D. P. Kingma and J. Ba, “Adam: A method for stochastic optimization,” in *Proceedings of the International Conference on Learning Representations*. OpenReview.net, 2015, pp. 1–15.
- [49] K. Papineni, S. Roukos, T. Ward, and W. Zhu, “Bleu: a method for automatic evaluation of machine translation,” in *Proceedings of the Annual Meeting of the Association for Computational Linguistics*. ACL, 2002, pp. 311–318.
- [50] C.-Y. Lin, “ROUGE: A package for automatic evaluation of summaries,” in *Text Summarization Branches Out*. Association for Computational Linguistics, 2004, pp. 74–81.
- [51] G. Zhang, S. Wei, H. Pang, and Y. Zhao, “Heterogeneous feature fusion and cross-modal alignment for composed image retrieval,” in *Proceedings of the International ACM Conference on Multimedia*. ACM, 2021, pp. 5353–5362.
- [52] G. Zhang, S. Wei, H. Pang, S. Qiu, and Y. Zhao, “Composed image retrieval via explicit erasure and replenishment with semantic alignment,” *IEEE Transactions on Image Processing*, vol. 31, pp. 5976–5988, 2022.
- [53] X. Chen, X. Song, G. Peng, S. Feng, and L. Nie, “Adversarial-enhanced hybrid graph network for user identity linkage,” in *Proceedings of the International ACM SIGIR Conference on Research and Development in Information Retrieval*. ACM, 2021, pp. 1084–1093.
- [54] L. van der Maaten and G. Hinton, “Visualizing data using t-sne,” *Journal of Machine Learning Research*, vol. 9, no. 86, pp. 2579–2605, 2008.